



# Sensitivity Analyses of Natural Convection in the AP1000 Passive Containment Cooling System Following LBLOCA Using CFD

June 2024

*Changing the World's Energy Future*

Hossam H. Abdellatif, David Arcilesi, Piyush Sabharwall, Palash Kumar Bhowmik



*INL is a U.S. Department of Energy National Laboratory operated by Battelle Energy Alliance, LLC*

#### **DISCLAIMER**

This information was prepared as an account of work sponsored by an agency of the U.S. Government. Neither the U.S. Government nor any agency thereof, nor any of their employees, makes any warranty, expressed or implied, or assumes any legal liability or responsibility for the accuracy, completeness, or usefulness, of any information, apparatus, product, or process disclosed, or represents that its use would not infringe privately owned rights. References herein to any specific commercial product, process, or service by trade name, trade mark, manufacturer, or otherwise, does not necessarily constitute or imply its endorsement, recommendation, or favoring by the U.S. Government or any agency thereof. The views and opinions of authors expressed herein do not necessarily state or reflect those of the U.S. Government or any agency thereof.

# **Sensitivity Analyses of Natural Convection in the AP1000 Passive Containment Cooling System Following LBLOCA Using CFD**

**Hossam H. Abdellatif, David Arcilesi, Piyush Sabharwall, Palash Kumar  
Bhowmik**

**June 2024**

**Idaho National Laboratory  
Idaho Falls, Idaho 83415**

**<http://www.inl.gov>**

**Prepared for the  
U.S. Department of Energy  
Under DOE Idaho Operations Office  
Contract DE-AC07-05ID14517**

# **Sensitivity Analyses of Natural Convection in the AP1000 Passive Containment Cooling System Following LBLOCA Using CFD**

**Hossam H. Abdellatif<sup>1</sup>, David Arcilesi<sup>1</sup>, Palash. K. Bhowmik<sup>2</sup>, Piyush Sabharwall<sup>2</sup>**

<sup>1</sup>University of Idaho, 1776 Science Center Dr, Idaho Falls, ID 83402, U.S.A.

<sup>2</sup>Idaho National Laboratory, 2525 Fremont Avenue, Idaho Falls, ID 83415-2209 U.S.A

## **ABSTRACT**

The AP1000 power plant has implemented multiple layers of passive safety systems to enhance reactor safety and ensure system integrity during postulated scenarios, such as loss of coolant accident (LOCA) and main steam line break (MSLB). Among these, the passive containment cooling system (PCCS) is a safety-related system designed to prevent the containment from exceeding the design limits of both pressure and temperature following a postulated design basis accident, by transferring heat from the steel containment vessel to the atmosphere. During LOCA, natural air convection plays a vital role in removing heat from the steel containment vessel to the atmosphere. This is integrated with the condensate film from the Passive Containment Cooling Water Storage Tank (PCCWST). Air natural convection is also the only heat removal mechanism after the dry-out of the PCCWST and during the loss of shutdown decay heat removal (LOSDHR) event. Therefore, it is essential to investigate the thermal hydraulics behavior of the containment under transient conditions to ensure its safety and integrity. This paper presents a simplified CFD/ANSYS FLUENT model developed to analyze the impact of different parameters, such as air relative humidity, air temperature, and steel containment temperature, on the natural convection capability to remove the decay heat following LOCA. The model aims to examine the thermal behavior of the containment and provides a comprehensive understanding of the system's natural convection capability during postulated accidents. The results obtained from the model can be used to improve the safety and integrity of the containment system and provide valuable insights for future research in the field.

*Keywords:* AP1000; Natural circulation; LOCA; Passive containment cooling system; CFD

## **1. INTRODUCTION**

The Passive Containment Cooling System (PCCS) plays a crucial role in ensuring the safety of AP1000. In the event of large break loss of coolant accidents (LBLOCA) or main steam line break (MSLB), the PCCS efficiently transfers heat from the containment shell to the atmosphere, thereby preventing the containment from exceeding the design pressure and temperature. The primary heat removal mechanisms in the AP1000 are water film, natural air circulation, and radiation heat transfer. Following LBLOCA, air cooling is supplemented by water film drains by gravity from the passive containment cooling water storage tank (PCCWST) situated atop the containment shield building [1]. This system is designed to operate automatically, without depending on any external power source or human intervention and is a key component in ensuring the safety of the system.

The removal of heat from a steel containment vessel (SCV) is possible via air natural circulation, albeit after 72 hours following a LBLOCA. Similarly, during a Loss of Shutdown Decay Heat Removal (LOSDHR) accident, heat can be removed via the same method. Air enters the annulus situated between the concrete shield building and the air baffle (downcomer). Air baffle plates are responsible for segregating

\* habdellatif@uidaho.edu

the downward flow from the upward flow in the riser, which subsequently cools the SCV and discharges via the stack. The riser itself is about 1/3 the width of the downcomer, which enhances the air velocity against the outer surface of the SCV. Figure 1 illustrates the various components of the Passive Containment Cooling System (PCCS) [2].

Several numerical simulations have been performed to investigate the AP1000 containment following postulated design basis accidents. The responses of the AP1000 containment during design basis accidents, including short-term double-ended hot leg (DEHL) break and MSLB, have been analyzed using the GOTHIC code [3-5]. A CFD model has been developed to study the air natural circulation and water falling film outside the AP1000 containment [6-7]. In this paper, a commercial CFD software, ANSYS FLUENT is employed to analyze the impact of air temperature, relative humidity, and steel temperature fluctuation on air cooling capability and PCCS performance in the event of water tank unavailability.

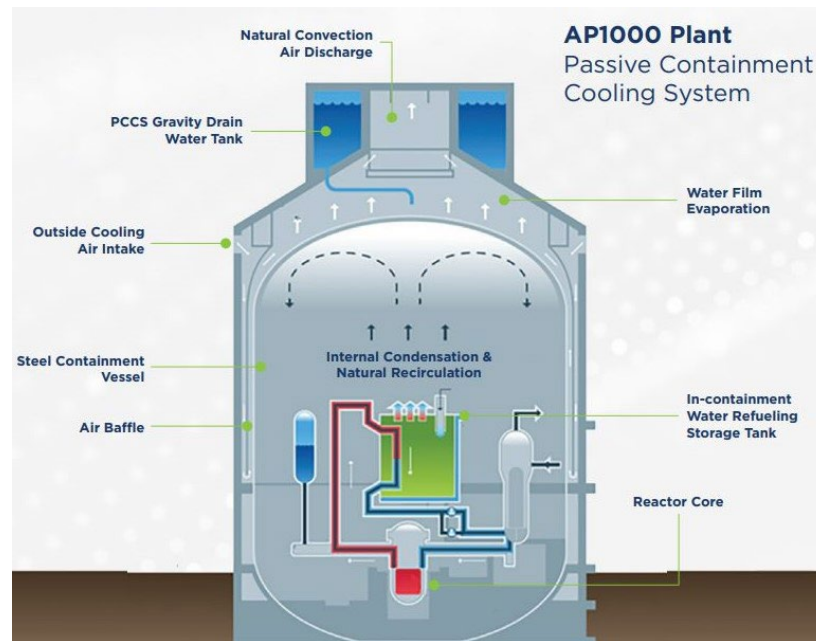


**Figure 1. The AP1000 passive containment cooling system.**

## **2. CFD MODEL**

### **2.1. Computational Domain**

Due to the fact that the AP1000 PCCS is an axisymmetric structure, a 20-degree sector is used to save computational time. The model includes the SCV surface, riser and downcomer with a simplified inlet, outlet, and air baffle with a turning vane. All dimensions are identical according to the latest update in the AP1000 DCD [8]. Figure 2 shows 2D and 3D sketches of the simplified model used in this study. Before constructing the CFD model, several underlying assumptions are considered.

- steady state conditions are assumed.
- The air-vapor mixture is treated as an ideal gas.
- PCCWST is disregarded.
- Radiation heat transfer is deemed negligible.
- Turning vanes have been incorporated into the model to ensure realistic air flow.

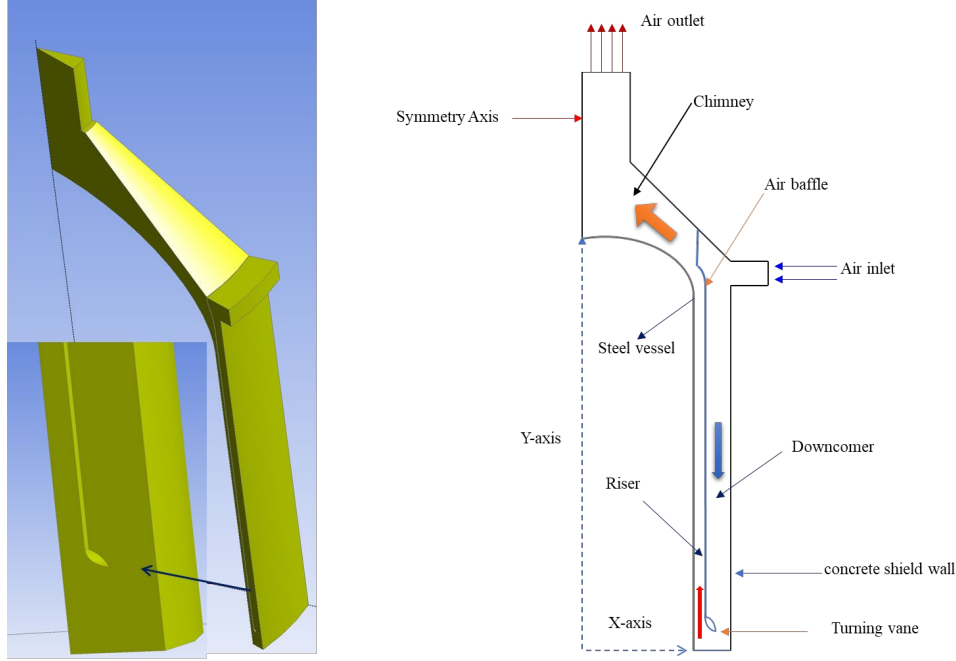


Figure 2. AP1000 PCCS simplified computational domain 3D model (left), 2D (right).

## 2.2. Mathematical Formulation

This study uses ANSYS FLUENT (2023 R2) to solve the steady-state governing equations including mass, momentum, and energy equations. Realizable  $k - \varepsilon$  turbulence model with enhanced wall treatment was adopted. Species and realizable  $k - \varepsilon$  turbulence model equations can be expressed as follows:

Continuity equation:

$$\frac{\partial}{\partial x_i} (\rho u_i) = S_m \quad (1)$$

Momentum equation with Reynolds stress employs Boussinesq hypothesis:

$$\frac{\partial}{\partial x_j} (\rho u_i u_j) = -\frac{\partial p}{\partial x_i} + \frac{\partial}{\partial x_j} \left\{ \mu \left( \frac{\partial u_i}{\partial x_j} + \frac{\partial u_j}{\partial x_i} - \frac{2}{3} \delta_{ij} \frac{\partial u_k}{\partial x_k} \right) \right\} + \frac{\partial}{\partial x_j} (-\rho \overline{u_i u_j}) + S_{mom} \quad (2)$$

Reynolds stress is given by:

$$-\rho \overline{u_i u_j} = \mu_t \left( \frac{\partial u_i}{\partial x_j} + \frac{\partial u_j}{\partial x_i} \right) - \frac{2}{3} \rho k \delta_{ij} \quad (3)$$

where  $\delta_{ij}$  is Kronecker delta.

Turbulent heat transport is modeled using the concept of Reynolds' analogy to turbulent momentum transfer and is described as:

$$\frac{\partial}{\partial x_i} \{(\rho E + p)u_i\} = \frac{\partial}{\partial x_j} \left\{ \kappa_{eff} \frac{\partial T}{\partial x_j} \right\} + S_{heat} \quad (4)$$

where  $E$  and  $\kappa_{eff}$  are total energy and effective thermal conductivity respectively.

The  $k$  and epsilon transport equations in the  $k - \varepsilon$  turbulence model are given by:

$$\frac{\partial}{\partial x_i}(\rho k u_i) = \frac{\partial}{\partial x_i} \left[ \left( \mu + \frac{\mu_t}{\sigma_k} \right) \frac{\partial k}{\partial x_i} \right] + G_k + G_b - \rho \varepsilon + Y_M + S_k \quad (5)$$

$$\frac{\partial}{\partial x_i}(\rho \varepsilon u_i) = \frac{\partial}{\partial x_i} \left[ \left( \mu + \frac{\mu_t}{\sigma_\varepsilon} \right) \frac{\partial \varepsilon}{\partial x_i} \right] + \rho C_1 S_\varepsilon - \rho C_2 \frac{\varepsilon^2}{k + \sqrt{\varepsilon \nu}} + C_{1\varepsilon} \frac{\varepsilon}{k} C_{3\varepsilon} G_b + S_\varepsilon \quad (6)$$

where  $G_k$ ,  $G_b$ ,  $Y_M$ ,  $S_k$ , and  $S_\varepsilon$ , represent the turbulent kinetic energy production due to the mean velocity gradients, buoyancy, fluctuation dilatation in compressible turbulence to the overall dissipation rate, and the user-defined source terms for  $k$  and epsilon, respectively.

The vapor species transport equation can be written as follows:

$$\frac{\partial}{\partial x_i}(\rho u_i Y_v) = \frac{\partial}{\partial x_i} \left[ \left( \rho D_{v,m} + \frac{\mu_t}{Sc_t} \right) \frac{\partial Y_v}{\partial x_i} \right] + S_v \quad (7)$$

where  $Y_v$ ,  $D_{v,m}$ ,  $Sc_t$ , and  $S_v$  represent vapor mass fraction, vapor mass diffusion coefficient, turbulent Schmidt number and vapor source term, respectively.

### 2.3. Computational Mesh

The study utilizes a tetrahedral mesh that features refinement in the near-wall regions. Figure 3 displays the mesh details at specific positions. The cells in the bulk have a typical size of 10 cm, and the total number of elements is 0.924 M. The first layer of cells adjacent to the walls is set with a width of 0.5 mm and an increasing ratio of 1.2. Additionally, 19 layers are established for the boundary. The grid independence is verified, and the results remain consistent despite further grid refinements.

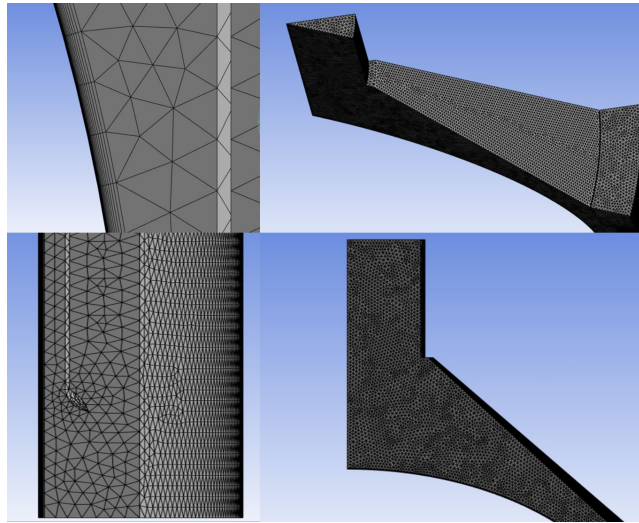


Figure 3. Computational mesh.

### 2.4. Boundary Conditions

When exploring natural convection, it is crucial to take into account the density of the fluid under investigation. In the annular region, where significant density variations occur, it is preferable to use an

ideal gas model instead of the Boussinesq density model. For the LBLOCA scenario, we assume that the steel vessel temperature is uniformly 150°C, while the relative humidity and temperature of the air are 22% and 25°C, respectively. The air baffle temperature is also set to 25°C. The inlet and outlet boundaries are established as pressure inlet and pressure outlet, respectively. In this study, we utilized an ANSYS FLUENT model that employs a pressure-based segregated solver with the SIMPLE algorithm, utilizing second-order upwind for spatial discretization and least square cell-based for gradient. The mixture properties of thermal conductivity and viscosity are determined by using the ideal gas mixing law since the density of the air-vapor gas mixture is treated as an ideal gas.

## 2.5. Sensitivity analysis parameters

In this study a series of sensitivity studies were performed to investigate their impact on the natural circulation and heat transfer capabilities in the absence of water film cooling. As mentioned above the base case represents the LBLOCA scenario with uniform temperature of steel vessel wall of 150°C and 22% relative humidity while the air temperature remains the same. First, the effect of steel vessel temperature variation has been studied for three different cases as shown in Table I. After that the vessel wall temperature is kept constant at LOCA scenario conditions and the air temperature and relative humidity have been changed to study their impact on the heat removal capability from the containment vessel as shown in Table II.

**Table I. Sensitivity analyses of vessel wall temperature variation.**

Parameter	T <sub>wall</sub> (°C)	RH (%)	T <sub>air</sub> (°C)
Case#1 (Base case)	150	22	25
Case#2	100	22	25
Case#3	50	22	25

**Table II. Sensitivity analyses of air temperature and relative humidity.**

Parameter	T <sub>wall</sub> (°C)	RH (%)	T <sub>air</sub> (°C)
Case#1 (Base case)	150	0	25
Case#2	150	50	25
Case#3	150	100	25
Case#4	150	22	15
Case#5	150	22	35
Case#6	150	22	45

## 3. Results and Discussion

The subsequent section outlines the main outcomes derived from the sensitivity studies conducted, which address the velocity and temperature fields in both the riser and downcomer. Additionally, the analysis encompasses the total wall heat flux. The scope of this paper limits the discussion to the first three cases presented in Table I, while the remaining sensitivity analysis will be included in a forthcoming publication. For base case which represents the LBLOCA scenario, the velocity contours within the air flow path of the PCCS are presented in Figure 4. In the downcomer air flow channel, the gas velocity remains constant at approximately 1.6 m/s, while in the riser air flow channel, the gas velocity ranges from 4 to 5.5 m/s with a mean value of 4.4 m/s. The gas velocity in the riser channel progressively increases along the flow direction



due to the higher wall temperature transferred to the gas. The average gas velocity reduces once again in the dome channel. The gas velocity remains around 5 m/s in the vicinity of the vessel wall, whereas it drops almost to less than 2 m/s in areas far from the vessel wall. Figure 5 depicts the temperature contours in the air flow path of the PCCS. In the downcomer channel, the gas temperature remains nearly constant.

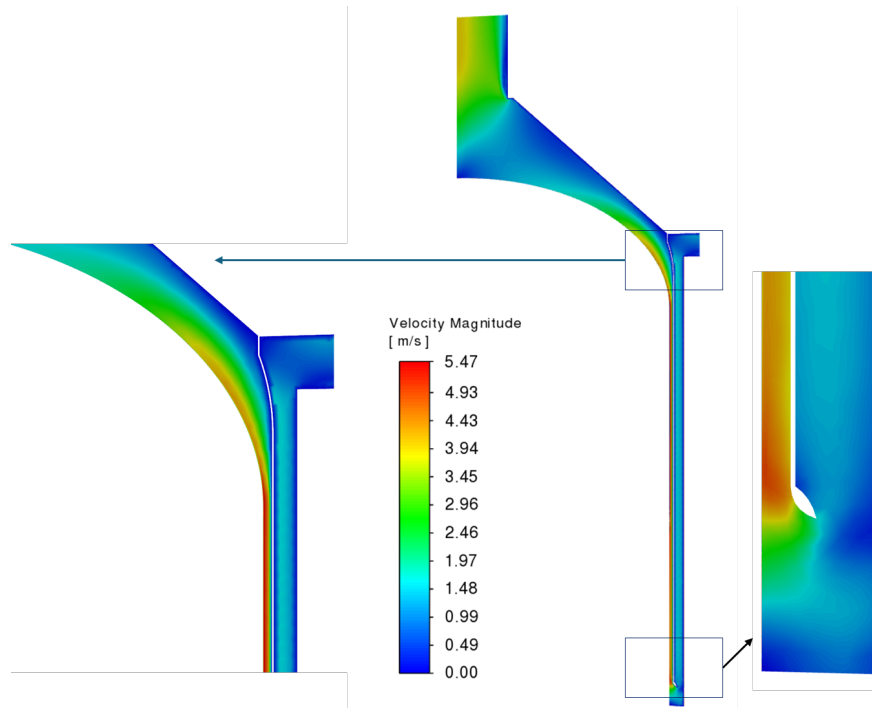


**Figure 4. Gas velocity contour in the PCCS air flow path.**

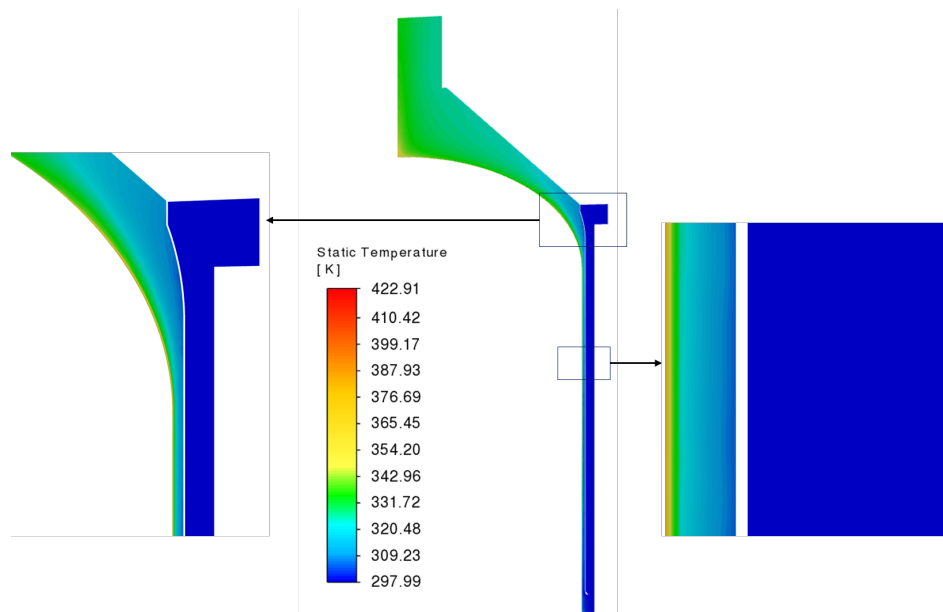


**Figure 5. Gas temperature contour in the PCCS flow path.**

Although the steel air baffle can conduct a small amount of heat to the downcomer channel, its impact is minimal. Conversely, in the riser channel, the gas is heated by the vessel wall, with the average temperature of the gas increasing from 298 K to 317 K in the channel. In the dome channel, the gas temperature continues to rise. While the temperature is relatively uniform in the bulk of the channel, the gas temperature near the wall ranging from 340 -350 K. At the chimney outlet, the average gas temperature is 327.7 K.

### 3.1. CFD model Validation

The current model has been validated against the available data through similar research and by utilizing the results obtained by the Westinghouse GOTHIC code for the AP1000 reactor [9]. For the sake of brevity, a comparison of steady state riser axial velocity corresponding to double-ended LBLOCA has been made between our CFD model and those presented in [5], [7], and [9]. The results demonstrate that our CFD model is in good agreement with the revised Westinghouse GOTHIC model when compared to the other models as shown in Figure 6.

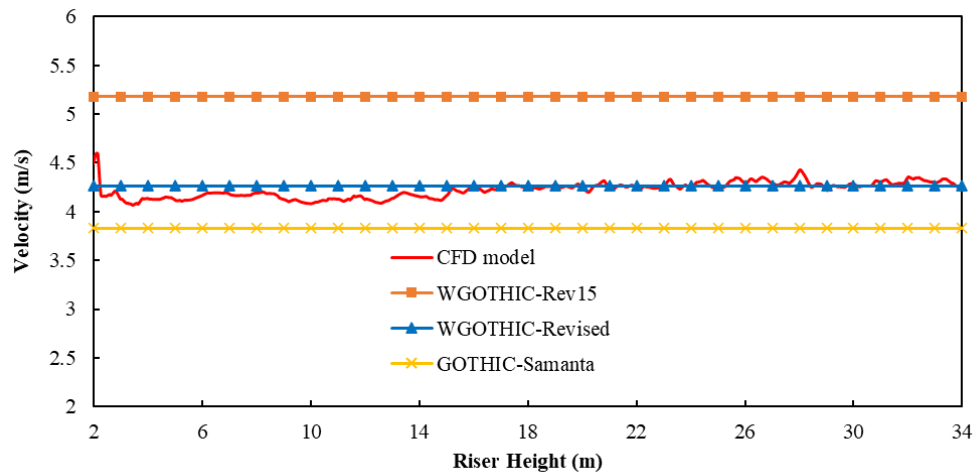


Figure 6. Riser velocity comparison with other models.

### 3.2. Sensitivity analyses results

The following subsection presents simulated results for three cases with different vessel wall temperatures. The velocity and temperature fields are introduced, along with the total heat transfer rate resulting from natural air convection only. Concerning the velocity field, it was observed that the gas velocity inside the riser increases with increasing the vessel wall and hence flow rate as shown in Figure 7. This refers to the fact that the high temperature of the steel containment vessel causes a decrease in local air density, resulting in enhanced buoyancy and upward flow. The mean velocity of gas for vessel wall temperatures of 150°C, 100°C, and 50°C were found to be 4.17 m/s, 2.68 m/s, and 1.82 m/s, respectively.

In relation to the gas temperature within the riser annulus, it is worth noting that an increase in vessel wall temperature results in a corresponding increase in the temperature transferred to the air, and conversely, a decrease in wall temperature leads to a reduction in the temperature transferred to the air as shown in Figure 8. It is observed that the maximum gas temperature in the riser for the three cases is 317 K, 312.87 K, and 303 K, respectively. Further, the average gas temperature in the middle of the riser is 307, 304.76 and 300.57 K, respectively.

Based on the simulated results, it was observed that when considering air natural convection only, the heat transfer capability increases with an increase in the vessel wall temperature. During LBLOCA, the heat transfer rate for the base case was found to be about  $6.35 \text{ MW}_{\text{th}}$ . On the other hand, when the vessel wall temperature decreases, the heat transfer rate also decreases. Results also show that the heat transfer rate for case #2 is about 3 MW, which is 50% less than the base case. For case #3, which is  $100^\circ\text{C}$  less than the base case, the heat transfer rate is approximately 40.778 kW, which is 99.35% less than the base case and 98.66% less than case #2 as shown in Figure 9.

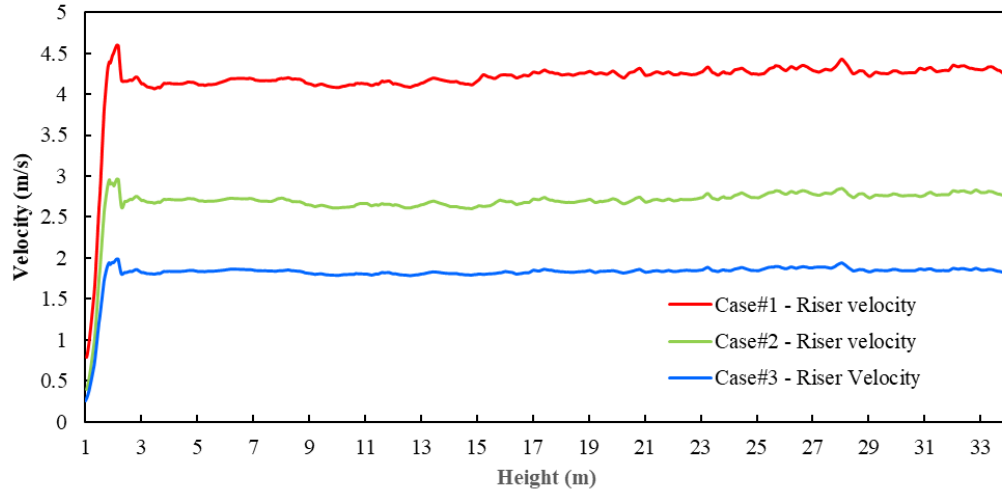


**Figure 7. Riser axial air velocity at three different wall temperature.**

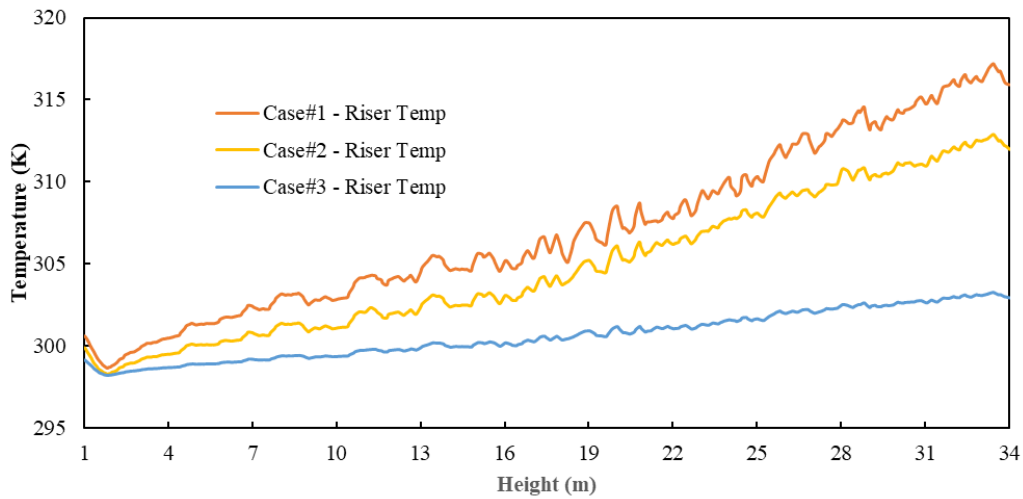


**Figure 8. Riser axial temperature at three different wall temperature.**

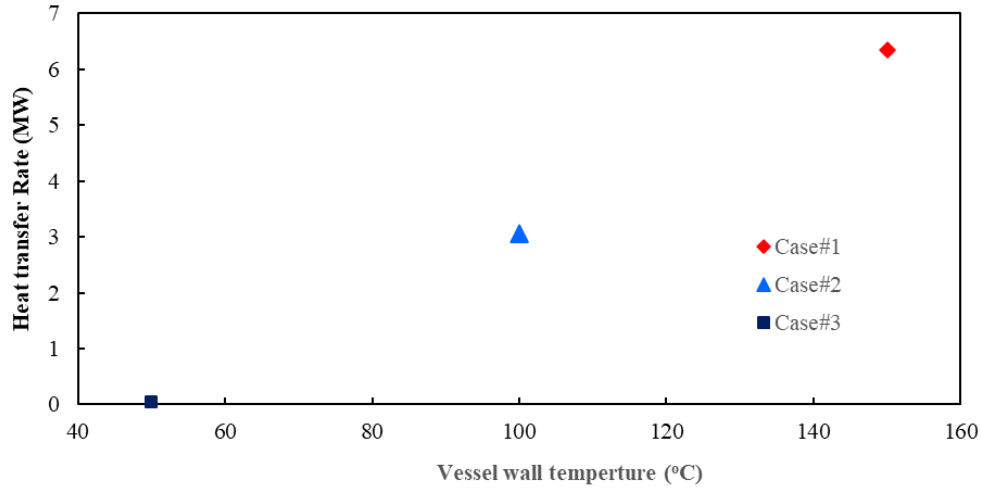


**Figure 9. Total heat transfer rate at different wall vessel temperature.**

#### 4. CONCLUSIONS

The present study employs a simplified CFD model to investigate the heat transfer performance of AP1000 passive containment cooling system (PCCS) when using air alone through a series of sensitivity analyses. The findings of these simulations are as follows:

- The base case represents the LBLOCA scenario, while case #3 represents the normal operation of the reactor at the vessel wall temperature of 50°C.
- Following the LBLOCA, the primary containment cooling water storage tank (PCCWST) has been depleted of its water resource after 3 days, leading to the absence of the primary cooling source for the steel containment. As a result, the heat removal process is primarily driven by natural air convection and radiation heat transfer.
- Excluding the fraction of decay heat removed by radiation, the external natural convection of air outside the containment is proficient in dissipating approximately 6MW of heat from the vessel containment.
- The velocity and temperature of air natural convection, as well as the heat removal power, are observed to increase with an increase in the outside surface temperature of steel containment. This trend indicates that the thermal performance of the steel containment system is directly proportional to its external surface temperature.
- The heat removed by air only is consistent with Westinghouse enhanced shield building design where our simulation results showed that during LBLOCA, air can remove up to 6 MW<sub>th</sub> of decay power.
- Without PCCWST, air natural convection cannot remove all decay power after LBLOCA.
- To mitigate the decay heat generated from LOCA scenarios, a more efficient optimization of the air flow path in the PCCS is necessary.
- Our CFD results are totally consistent with Westinghouse GOTHIC code and available research data.

## ACKNOWLEDGMENTS

This research was funded by United State (U.S.) Department of Energy (DOE) Advanced Reactor Demonstration Project (ARDP) program office grant number ARDP-20-23819. Funding Opportunity Number DE-FOA-0002271, Risk Reduction Pathway. The authors would like to thank the U.S. DOE National Reactor Innovation Center (NRIC) ARDP program office and Irradiation Experiment and Thermal Hydraulics Analysis Department at Idaho National Laboratory (INL) for the encouragement and support.

## REFERENCES

- [1] T. L. Schulz, “Westinghouse AP1000 advanced passive plant,” *Nuclear Engineering and Design*, vol. 236, no. 14–16, pp. 1547–1557, Aug. 2006.
- [2] R. Wright, H. Xu, M. Durse, and T. Sutton, “Analysis of the AP1000® passive containment cooling system air flow path using computational fluid dynamics.
- [3] Z. Huang, Yuh-Ming Ferng, W. S. Hsu, B.-S. Pei, and Y.-S. Chen, “Analysis of AP1000 containment passive cooling system during a loss-of-coolant accident,” *Annals of Nuclear Energy*, vol. 85, pp. 717–724, Nov. 2015.
- [4] K. Fernández-Cosials, Zuriñe Goñi, Gonzalo Jiménez Varas, and J. L. Montero, “Three-dimensional simulation of a LBLOCA in an AP1000 ® containment building,” *Energy Procedia*, vol. 127, pp. 234–241, Sep. 2017.
- [5] Samanta Estévez-Albuja, K. Fernández-Cosials, C. Vázquez-Rodríguez, Zuriñe Goñi-Velilla, and Gonzalo Jiménez Varas, “AP1000 Passive Containment Cooling System study under LBLOCA conditions using the GOTHIC code,” *Nuclear Engineering and Design*, vol. 384, pp. 111442–111442, Dec. 2021.
- [6] G. Jimenez, Z. Goñi, G. Del Río, S. Estévez, and C. Queral, “AP1000 ® Passive Cooling Containment Analysis with Computational Fluid Dynamics Codes.” Accessed: Jan. 13, 2024.
- [7] X. Wang, H. Chang, M. L. Corradini, T. Cong, and J. Wang, “Prediction of falling film evaporation on the AP1000 passive containment cooling system using ANSYS FLUENT code,” *Annals of Nuclear Energy*, vol. 95, pp. 168–175, Sep. 2016.
- [8] NRC: Package ML11171A500, “Westinghouse AP1000 Design Control Document Rev. 19,”.
- [9] NRC, “Evaluation of the Effect of the AP1000® Enhanced Shield Building Design on the Containment Response and Safety Analyses,” Accessed: Jan. 15, 2024.